3.2 Species-level phylogeny of Sericini in the Himalaya

3.2.1 The phylogeny of *Maladera* (subgenus *Cycloserica*)

Material and methods

Taxon sampling and characters

Twenty species belonging to *Comaserica*, *Euserica*, *Leucoserica*, *Pleophylla*, *Stilbolemma*, and six separate species' groups of *Maladera* (subgenus *Amaladera*, *Cephaloserica*, *Cycloserica*, *Macroserica*, *Maladera*, and *Omaladera*) were included in the cladistic analysis. *Pleophylla* sp. was chosen as the outgroup taxon due to still insufficient knowledge about the relationships of the taxa of *Maladera* to other Sericini possessing the apomorphies of 'modern' Sericini (chapter 3.1). *Comaserica* and *Pleophylla* are with high probability (chapter 3.1) not part of the ingroup since they do not share the apomorphic character states of 'modern' Sericini. Character description and coding was based on 20 species belonging to seven genera (see appendix A 3.2.1).

Phylogenetic analysis

The 37 characters (28 binary and 9 multistate) were all unordered and equally weighted. Inapplicable characters were coded as "-", while unknown character states were coded as "?" (Strong and Lipscomb 1999). The parsimony analysis was performed in NONA 2.0 (Goloboff 1999) using the parsimony ratchet (Nixon 1999) implemented in NONA, run with WINCLADA vs. 1.00.08 (Nixon 2002) as a shell program. Two hundred iterations were performed (one tree hold per iteration). The number of characters to be sampled for reweighting during the parsimony ratchet was determined to be three. All searches were done under the collapsing option "ambiguous" which collapses every node with a minimum length of 0.

Bremer support (Bremer 1988, 1994) and bootstrap values (Felsenstein 1985) were evaluated using NONA. Bootstrap analyses of data were performed with 200 replicates using TBR branch swapping. The search was set to a Bremer support level of 12 (based on the number of unambiguous character changes for each node given by WINCLADA), with seven runs (each holding a number of trees from 100 to 500 times multiple of suboptimal tree length augmentation) and a total hold of 8000 trees. Character changes were studied and mapped on the tree using WINCLADA.

Characters and character states

In describing character states, I refrain from formulating any hypothesis about their transformation. In particular, coding does not imply whether a state is derived or ancestral. The data matrix is presented in appendix B 3.2.1.

Head

1. *Labroclypeus, anterior margin medially*: (0) not reflexed and produced into a lobe (Figs 33C,D); (1) strongly reflexed and produced into a lobe or tooth (Fig. 33A).
2. *Labroclypeus, lateral margin*: (0) not angularly widened (Figs 33C,D); (1) angularly widened (Fig. 33A).
3. *Labrum medially*: (0) not or only weakly sinuate (Figs 33C,D); (1) deeply concavely sinuate (Fig. 33B).
4. *Frons*: (0) entirely setose; (1) completely glabrous at middle; (2) with a transverse row of setae behind the middle; (3) with a row of setae behind frontoclypeal suture.

Fig. 33. A, M, R, Z-Bb: *Maladera quinquidens*; **B, W, X:** *M.* (*Cycloserica*) *excisipes*; **C, H, K, L, U:** *M. holosericea*; **D:** *M. himalayica himalayica*; **E:** *M. taurica*; **F:** *M. mechiana*; **G, N, P, Q, V, Y:** *Leucoserica arenicola*; **J, T:** *M. insanabilis*; **O:** *Nipponoserica koltzei*; **S:** *Pleophylla* sp. **A:** head cranial view; **B:** head ventral view; **C, D:** head dorsal view (left half); **E-G:** habitus, dorsal view; **H, J:** width of meso- and metasternum between the mesocoxae; **K:** apical margin of elytra; **L, M**: metacoxa with its medial process (white arrow), ventral view (**L**, trochanter and metafemur removed); **N, O:** metafemur, ventral view; **P, S:** metatibia, ventral view; **T, U:** metatarsomeres, ventral view; **V:** aedeagus, lateral view; **W, X, Bb:** parameres, dorsolateral view; **Y:** parameres, lateral view; **Z:** parameres, dorsal view; **Aa:** apex of aedeagus, dorsal view (not to scale).

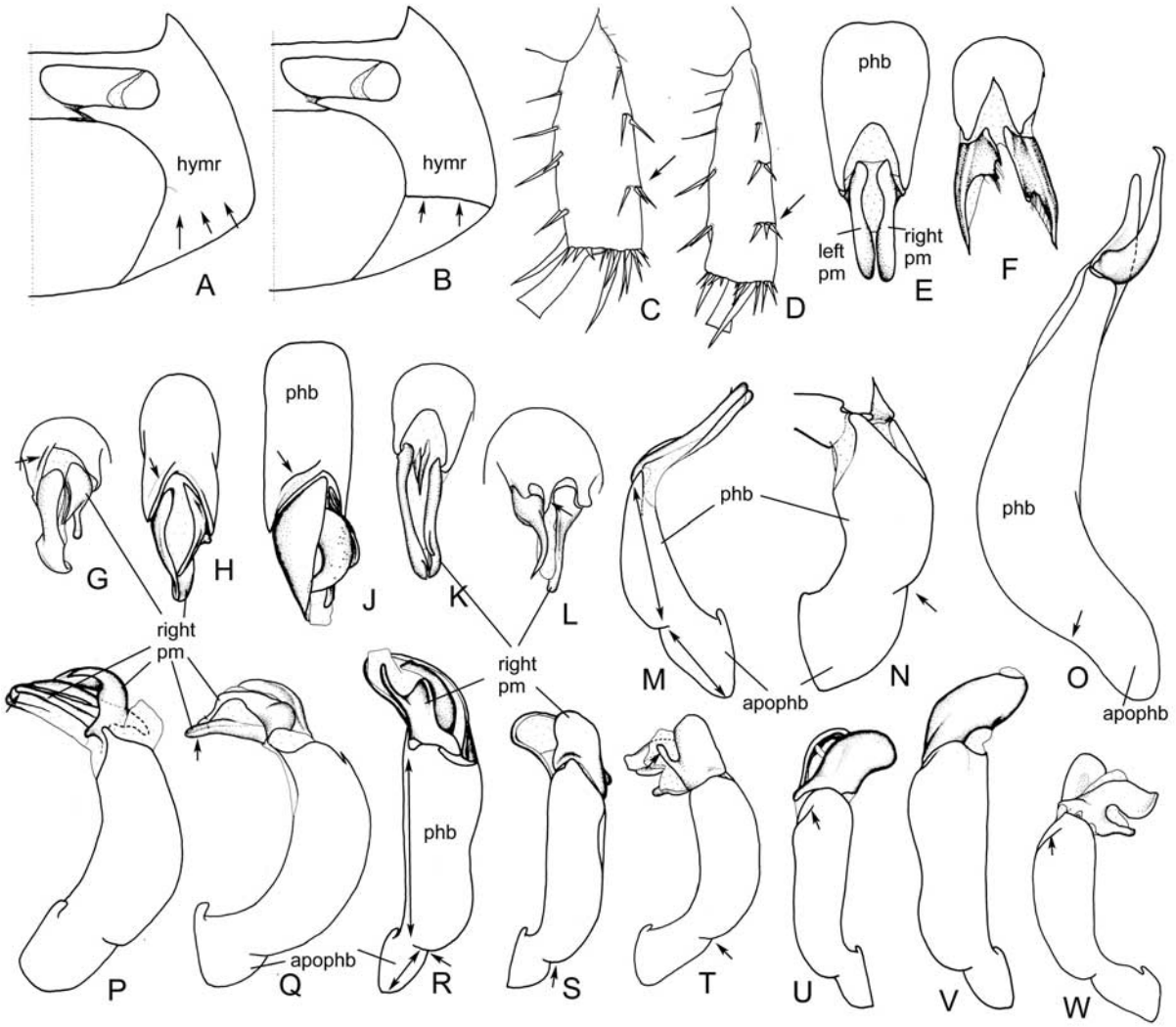

Fig. 34. A: *Hyposerica* sp.; **B:** *Maladera simlana*; **C, O:** *M. insanabilis*; **D:** *M. himalayica himalayica*; **E:** *Stilbolemma sericea*; **F, N:** *Pleophylla* sp.; **G, T, W:** *M. caspia*; **H, S, U:** *M. kerleyi*, **J, R, V:** *Maladera quinquidens*; **K, M:** *M. holosericea*; **L:** *M. cariniceps*; **P:** *M. farsensis*; **Q:** *M. taurica*. **A, B:** prothorax, ventral view; **C, D:** metatibia, lateral view; **E-L:** parameres, dorsal view; **M, O, U-W:** aedeagus, left side lateral view; **N, P-T:** aedeagus, right side lateral view (not to scale).

5. *Lateral margin of labroclypeus produced with ocular canthus into*: (0) a distinct angle (Fig. 33C); (1) a blunt indistinct angle (Fig. 33D).
6. *Labium, prementum*: (0) flat (Fig. 33B); (1) apically strongly elevate (Fig. 33A); (2) apically weakly elevate.
7. *Antenna, number of antennomeres*: (0) ten; (1) nine.
8. *Dorsal surface of body, coloration*: (0) blackish brown (Fig. 33E); (1) reddish brown (Fig. 33F); (2) yellowish (Fig. 33G); (3) 0&1.

Thorax

9. *Pronotum, basal marginal line*: (0) at least in parts present; (1) completely absent.
10. *Prothorax, hypomeron ventrally*: (0) not carinate (Fig. 34A); (1) carinate (Fig. 34B).
11. *Elytra, apical margin*: (0) glabrous; (1) with microtrichomes (Fig. 33K).
12. *Mesosternum between mesocoxae*: (0) broad (Fig. 33J); (1) narrow (Fig. 33H).

Legs

13. *Metacoxa, posterior margin*: (0) glabrous or simply setose; (1) finely covered by microtrichomes (Fig. 33M).

14. *Metacoxa, medial process*: (0) wide and rounded apically (Fig. 33L); (1) pointed apically (Fig. 33M).
15. *Metafemur, posterior margin dorsally*: (0) completely smooth; (1) serrate in apical half; (2) completely serrate.
16. *Metafemur, anterior margin in distal half*: (0) weakly convex (Fig. 33O); (1) strongly convex (Fig. 33N).
17. *Metatibia, dorsal margin*: (0) longitudinally convex (Figs 33P,Q,S); (1) sharply margined (Fig. 33R); (2) weakly margined in parts.
18. *Metatibia, posterior group of robust setae on dorsal margin*: (0) at apical third or more distal (Figs 33R,S, 34C,D); (1) shortly behind the middle of metatibia (Fig. 33P,Q).
19. *Metatibia, ventral margin*: (0) without serrated keel (Fig. 33P); (1) with serrated keel.
20. *Metatibia, basal external group of spines*: (0) at 1/3 or less of metatibial length; (1) at half of metatibial length.
21. *Metatibia, medial face*: (0) without punctures or setae (Fig. 33R, grey arrow); (1) with coarse punctures dorsally bearing a seta (Fig. 33P, grey arrow).
22. *Metatarsomeres ventrally*: (0) setose (Fig. 33U); (1) glabrous (Fig. 33T).
23. *Protarsus, basal tooth of interior claw*: (0) simply pointed in the tip; (1) lobiform.

Male genitalia

24. *Phallobase*: (0) symmetrical (Figs 34E,F); (1) asymmetrical (Figs 33V,Z, 34G-L).
25. *Phallobasal apodeme*: (0) not or weakly reduced in size (smallest ratio phallobasal apodeme/ distal portion of phallobase: 0.27) (Figs 34M,N); (1) strongly reduced in size (largest ratio phallobasal apodeme/ distal portion of phallobase: 0.14) (Figs 33V, 34O,R-W).
26. *Phallobase (ratio length of phallobase/ length of body)*: (0) not elongate (0.2) (Figs 34M,N,P,Q); (1) moderately elongate (0.3-0.34) (Figs 34R-W); (2) strongly elongate (> 0.39) (Fig. 34O).
27. *Phallobase, incision between phallobasal apodeme and distal portion of phallobase*: (0) weak (Figs 34M-Q,T); (1) strong (Figs 34R,S).
28. *Phallobase, at apex dorsomedially*: (0) deeply and concave sinuate (Figs 34E,F,K); (1) in respect to base of parameres almost not sinuate (Figs 33W,Z, 34G-J); (2) margin triangularly produced at middle (Fig. 34L).
29. *Phallobase, at apex ventromedially*: (0) deeply sinuate; (1) almost not sinuate.
30. *Phallobase, distal portion (lateral view)*: (0) at maximum half of its length subequal in width (Figs 34M-Q); (1) at least four fifths of its length subequal in width (Figs 33V, 34R-W).
31. *Phallobase, preapical fold at left side of apex dorsolaterally*: (0) absent (Figs 34E,F,K,L); (1) present (Figs 33V,W,Z,Bb, 34G-J); (2) 0&1.
32. *Phallobase, insertion of parameres (lateral view)*: (0) freely visible (Figs 34M-Q); (1) covered by laterally produced phallobase (Figs 33V,W,Y,Bb, 34R-W).
33. *Right paramere*: (0) simple; (1) at base widened lobiformly; (2) divided into two lobes of almost same size.
34. *Left paramere*: (0) simple; (1) at base widened lobiformly; (2) divided into two lobes of almost same size.
35. *Ventral lobe of parameres*: (0) widely separate (Figs 33W,Y, 34T); (1) closely attached (Figs 34P,Q).
36. *Equivalent of the ventral lobes of both parameres*: (0) curved dorsally (Figs 34V,W, 34T); (1) straight (Figs 34P,Q).
37. *Parameres laterally*: (0) smooth, without minute teeth (Fig. 33Bb); (1) parts of surface completely or partly with minute teeth (Figs 33X,Y).

Results

The analysis of 37 adult characters with the parsimony ratchet using the above mentioned settings and repeating the search ten times yielded three equally parsimonious trees of 79 steps (ensemble consistency index (CI): 0.62, ensemble retention index (RI): 0.79). In addition to the character description, for each character the consistency index (CI) and the retention index (RI) calculated by WINCLADA analysis are given in appendix C 3.2.1. The strict consensus of these trees is presented in Figure 35 with areas of conflict in topology shown as polytomies.

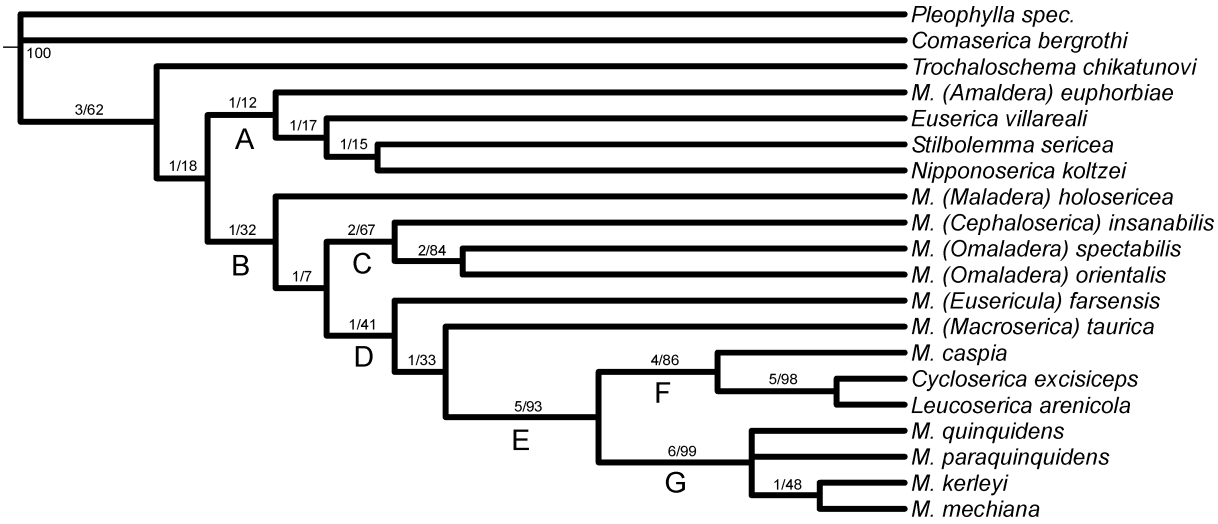

Fig. 35. Strict consensus (79 steps, CI: 0.62, RI: 0.79) of the 3 equally parsimonious trees with a length of 79 steps (CI: 0.62 and RI: 0.79); above each branch support indices (Bremer support/ bootstrap values) (*M.* = *Maladera*).

The strict consensus tree (Fig. 35) of equally weighted characters is best resolved in basal as well as in apical nodes. Two major lineages may be recognized from the strict consensus tree (Fig. 35) within the ingroup: the first including *Maladera* (subgenus *Amaladera*), *Euserica*, *Nipponoserica*, and *Stilbolemma* (node A); the second (node B) comprises the *Maladera* species of the subgenera *Maladera*, *Cephaloserica*, and *Omaladera*, furthermore *M. caspia*, and the taxa of the *M. quinquidens*-group (Ahrens 2004b; node G) as well as the taxa so far assigned to *Cycloserica* and *Leucoserica*. Monophyly of the taxa, so far classified as *Maladera*, was not apparent according to the tree topology. Branch support values of most basal nodes were rather low. Rather well supported relationships are the sister taxon relationship of *Cephaloserica* + *Omaladera* (node C, Bremer support: 2, bootstrap value: 67 %), found also in chapter 3.2.2 and the monophyly of the *Maladera* subgenus *Omaladera*, represented here by *M. orientalis* and *M. spectabilis*. Moreover, best supported was the sister taxon relationship (node E, Bremer support: 5, bootstrap value: 93 %) of the *M. quinquidens*-group (node G) and a Middle Asian clade (node F, Bremer support: 4, bootstrap value: 86 %) comprising *M. caspia* (*Cycloserica excisipes*, *Leucoserica arenicola*). The only ambiguous topology was within the *M. quinquidens*-group, showing polytomy in (*M. quinquidens*, *M. paraquinquidens*, *M. kerleyi* + *M. mechiana*).

Discussion

Evaluation of the clades and implications on taxonomy of Maladera

The monophyly of the node E is one of the best supported branches, being based upon the following unambiguous apomorphies: (1) phallobase at apex dorsomedially in respect to base of parameres almost not sinuate (28:1); (2) distal portion of phallobase (lateral view) at least four fifths of its length subequal in width (30:1); (3) phallobase, preapical fold at left side of apex of dorsolateral phallobase present (31:1); (4) insertion of parameres (lateral view) covered by the laterally produced phallobase (32:1); and (5) ventral lobe of parameres widely separate (35:0). Since *Cycloserica* and *Leucoserica* have been treated for long time as well defined 'genera' (Reitter 1896, Medvedev 1952b), it was rather surprising, that *Cycloserica* and *Leucoserica* nested in the clade E with taxa assigned so far to *Maladera*. However, after Nikolaev (1987) synonymized correctly the two species, *L. arenicola* Solsky, 1876 and *L. diluta* Reitter, 1896, both *Leucoserica* and *Cycloserica*, have become monotypic. In addition, Nikolaev (1977) classified the latter name as a subgenus of *Maladera*. Outstanding diagnostic characteristics of both taxa could not be considered for the cladistic analysis, since most of them are simply autapomorphies of each of the species, *Cycloserica excisipes* and *Leucoserica arenicola*. Numerous apomorphies support the very close relationship of both taxa with *Maladera caspia* (node F, Fig. 36). Among those not subject to homoplasy are (1) the posterior group of robust setae on dorsal margin of metatibia is situated closely behind the middle of metatibia (18:1), and (2) the parameres, laterally finely covered with minute teeth (37:1). Due to sister taxa relationship of *Cycloserica* and *Leucoserica*, both nested deeply within the taxa of *Maladera* (node sequence B, D, E, F), it seems reasonable to consider both synonymous with *Maladera*. One of the two names (I suggest *Cycloserica* Reitter, 1896), being both of equal nomenclatural priority, might be used to name the clade of the node E, if ranked, as done here, as a genus group taxon (e.g. subgenus) (Fig. 36). From this conclusion result: *Maladera* (*Cycloserica*) *arenicola* (Solsky, 1876) comb. n. and *Cycloserica* Reitter, 1896 (=*Leucoserica* Reitter, 1896, syn. n.).

Results of present analysis reveal (Fig. 35), that *Maladera* is paraphyletic according to the present definition of the genus (Baraud 1992, Nikolaev 2002). *Euserica* (*Nipponoserica* + *Stilbolemma*) form a monophyletic clade with *Maladera* (*Amaladera*) *euphorbiae*. The resulting sister taxon to the clade comprises all other *Maladera* species included in the present analysis. Considering the large number of taxa which are assigned to *Maladera*, I retain it premature to draw any conclusions regarding the taxonomy and classification of these taxa. This should be reserved for a comprehensive cladistic analysis of *Maladera* based on a complete taxonomic revision of all its potential species.

The effect of the Alpine Tertiary orogenesis for the Maladera (Cycloserica) clade

The ranges of the taxa of the subgenus *Cycloserica* exhibit in comparison to all other groups of Sericini inhabiting the Himalaya a divergent pattern. The two principal clades (Fig. 37) are restricted to lowlands and colline regions, at both sides of Tertiary Alpine-Himalayan belt. While the *M. quinquidens*-group is restricted to the southern slope of the Himalaya and the small areas south of the Gangetic plain of the northern Indian subcontinent, *M. caspia*, *M. arenicola*, and *M. excisipes*, are adapted to the arid steppe and semi-desert climate of Middle Asia northerly of the Tertiary Alpine-Himalayan belt.

In connection with East Mediterranean ranges of the lineages (*Eusericula*, *Macroserica*) basal to the *Cycloserica* clade, a formerly 'circum-Paratethys' or at least southern 'Paratethys' distribution of the stem lineage of each of the lineages would be most consistent with their present ranges. However, due to lack of fossils of relevant lineages in these areas, it hardly can be stated definitely, whether the division of the lineages of *Cycloserica* has been caused by vicariance or by dispersal. Vicariance requires that taxa in the two areas and the barriers between them are the same age; whereas dispersal always assumes that the barrier predates the taxa (Siebert 1992).

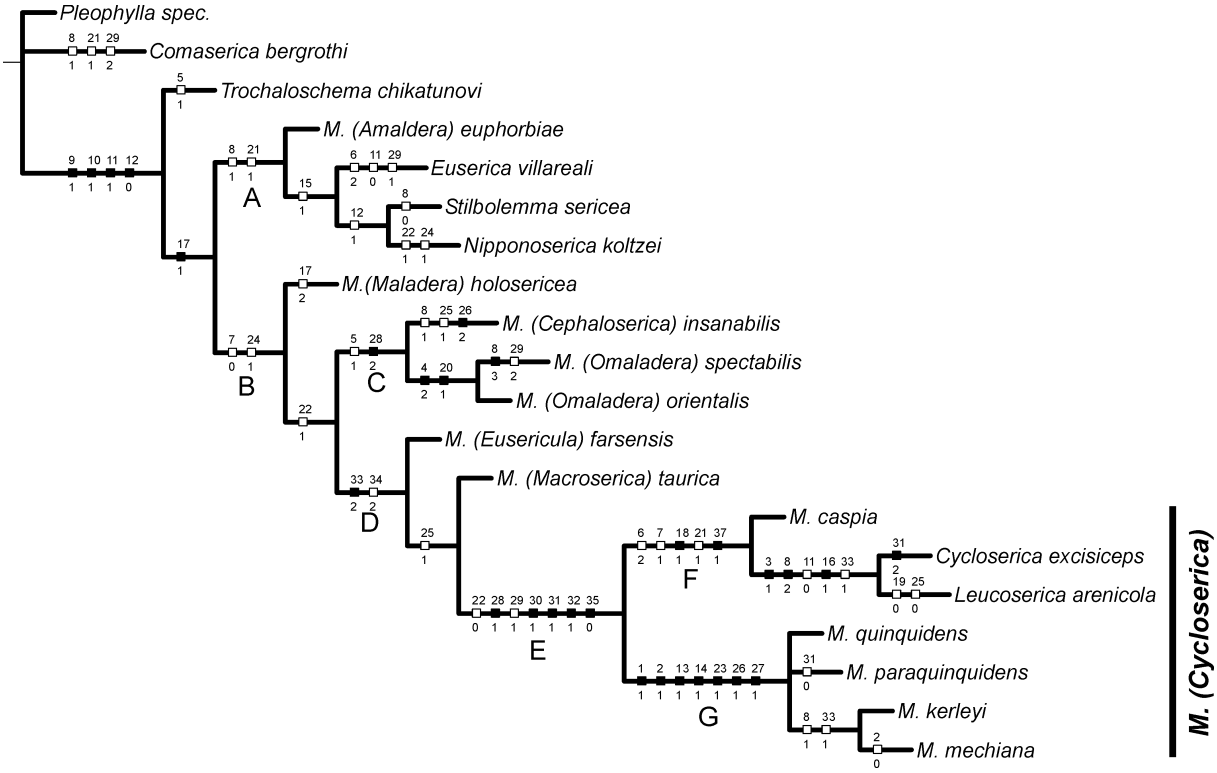

Fig. 36. Strict consensus (79 steps) tree of three MPTs (79 steps) resulting from parsimony ratchet with unweighted characters showing apomorphies mapped by state (discontinuous characters are mapped as homoplasy and only unambiguous changes are shown, unsupported nodes collapsed and using proportional branch lengths) (full squares: non-homoplasious character states; empty squares: homoplasious character states). (*M.* = *Maladera*)

Assuming vicariance as the driving force for splitting of the two principal *Cycloserica* lineages (node F,G), the oldest efficient barrier between the south-west Asian lowlands and Southern Asia was evident with the uplift of the Iranian Plateau. The Iranian Plateau has been uplifting for the last 5 Ma (Sborshchikov et al. 1981), forming three major mountain chains: (1) west of the Caspian Sea, the Lesser Caucasus of the Iranian Plateau connecting to the Greater Caucasus; (2) the Elburz Range of Iran situated directly south of the Caspian Sea; (3) the Kopet-Dagh and Balkhan mountains of Turkmenistan and northeast Iran rising to the east of the Caspian Sea.

However, the progressed climatic differentiation of Asia due to advanced uplift of the Himalaya and the Tibetan Plateau (Tapponier et al. 2001) makes it rather unlikely, that geographical isolation by the uplift of the Iranian Plateau was 'that event' leading to the splitting between nodes F and G. Since at least 8 Ma a monsoon climate was dominant in all Southern Asia (Prell et al. 1992, Quade et al. 1989), and due to retreat of Paratethys since Miocene the climate in Middle and Central Asia became more and more arid (Guo et al. 2002; Ramstein et al. 1997). Based on geological evidence, that first higher elevations (with barrier effect northerly) in the region of the present Himalaya and the Tibetan Plateau were achieved during Oligocene (Tapponier et al. 2001; Harrison et al. 1998), a more likely hypothesis is that the two *Cycloserica* lineages (node F and G) existed before they dispersed into the two separated areas (Fig. 37), the northern Indian subcontinent and the Middle Asian lowland.

While most of the lowland of Middle Asia during Palaeocene and Eocene was covered by sparse tropical savannah, its climate became colder in the late Eocene and a zone of true deserts was established (Atamuradov 1994). With the intensive tectonic movement during Neogene, lowlands of middle Asia underwent uplift, and due to transgression and regression of the sea, islands emerged occasionally (Atamuradov 1994), which later formed mountain

ranges such as Kopet-Dagh and Elburz. These fluctuations of land-sea distribution presumably offered fertile conditions for species diversification for the lineage of Middle Asian *Cycloserica* (node F). Since Early Pliocene the sea liberated completely most of Turkmenistan (Atamuradov 1994), allowing almost free dispersal of the lowland fauna.

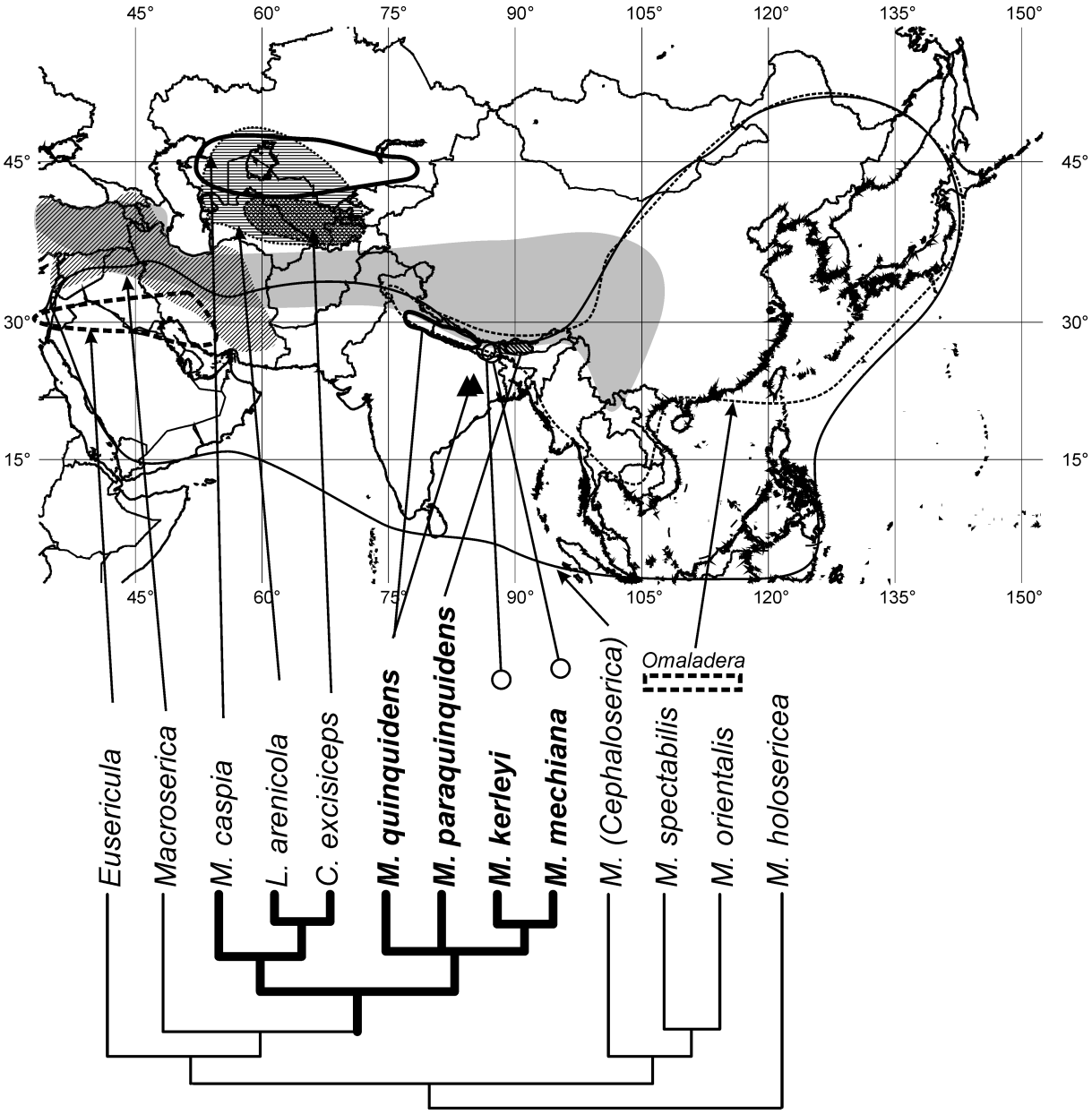

Fig. 37. Phylogeny of *Maladera (Cycloserica)* (indicated by bold tree branches) in its geographical framework, with indicated generalized distribution of their taxa and its related lineages (indicated by narrow tree branches). Subgenera names and corresponding cumulative ranges of all their included taxa were used (instead of the respective species of the subgenus included into the analysis) to generalize the evolutive scenario. To point out the position of the generic names *Cycloserica* (= *C.*) and *Leucoserica* (= *L.*), both synonymous with *Maladera*, these names have been retained for this illustration. (The Alpine Tertiary orogenic belt discussed as barrier is grey shaded; *M.* = *Maladera*).

The results presented here, although beginning to reveal an overall phylogenetic framework for *Maladera* that is relatively robust, as well as suggesting a number of well supported species relationships, are still very far from satisfactory regarding the completeness and the capacity to generate data with a temporal dimension, as for example provide molecular studies.